NAWCWPNS TP 8212

A Colocated Magnetic Loop, Electric Dipole Array Antenna (Preliminary Results)

by
P. L. Overfelt
D. R. Bowling
D. J. White
Research Department

SEPTEMBER 1994

NAVAL AIR WARFARE CENTER WEAPONS DIVISION
CHINA LAKE, CA 93555-6001

Approved for public release; distribution is unlimited.

Naval Air Warfare Center Weapons Division

FOREWORD

This report presents the electromagnetic analysis of a colocated electric dipole, magnetic loop antenna array. This work was performed at the Naval Air Warfare Center Weapons Division, China Lake, CA, during fiscal year 1994 in support of the IR Project on "Analysis of Electrically Small Antennas," and also in support of an accelerated technology initiative investigating high temperature superconducting antennas, sponsored by the Office of Naval Research, Information, Electronics, and Surveillance Science and Technology Department (ONR31). This work was monitored initially by Dr. Y. S. Park and subsequently by Dr. Donald H. Liebenberg under fund document N0001494WX35177.

This report is a working document subject to change and was reviewed for technical accuracy by Anna M. Martin.

Approved by
R. L. DERR, *Head*
Research Department
September 1994

Under authority of
D. B. McKinney
RAdm., U.S. Navy
Commander

Released for publication by
S. HAALAND
Deputy Commander for Research and Development

NAWCWPNS Technical Publication 8212

Published by . . . . . Technical Information Department
Collation . . . . . Cover, 16 leaves
First printing . . . . . 65 copies

REPORT DOCUMENTATION PAGE

Form Approved
OMB No. 0704-0188

1. AGENCY USE ONLY *(Leave blank)*	2. REPORT DATE	3. REPORT TYPE AND DATES COVERED
	September 1994	Interim - October 1993-September 1994

4. TITLE AND SUBTITLE
A COLOCATED MAGNETIC LOOP, ELECTRIC DIPOLE ARRAY ANTENNA (PRELIMINARY RESULTS)

5. FUNDING NUMBERS
N00014-94-WX-35177
N00014-94-WX-41012

6. AUTHOR(S)
P. L. Overfelt, D. R. Bowling, D. J. White

7. PERFORMING ORGANIZATION NAME(S) AND ADDRESS(ES)
Naval Air Warfare Center Weapons Division
China Lake, CA 93555-6001

8. PERFORMING ORGANIZATION REPORT NUMBER
NAWCWPNS TP 8212

9. SPONSORING/MONITORING AGENCY NAME(S) AND ADDRESS(ES)
Dr. Yoon Soc Park
ONR 44GI
Office of Naval Research
Washington, DC

10. SPONSORING/MONITORING AGENCY REPORT NUMBER

11. SUPPLEMENTARY NOTES

12A. DISTRIBUTION/AVAILABILITY STATEMENT
A Statement; Distribution Unlimited

12B. DISTRIBUTION CODE

13. ABSTRACT *(Maximum 200 words)*

(U) We present a detailed electromagnetic analysis of an electrically small colocated electric dipole and magnetic loop antenna array. This antenna is the simplest example of the Grimes multipole class of antenna arrays. We have determined that since the interaction term between the two elements disappears from the radial complex power, we were able to set the radial reactance to zero by choosing appropriate current magnitudes and phases on the array elements. By driving the two elements in quadrature, we obtained a much increased radiation intensity and directivity as well as increased radiated power.

14. SUBJECT TERMS	15. NUMBER OF PAGES
Antennas, Mutual Impedance, Electric Dipole, Arrays, Multipoles, Magnetic Loop	32
	16. PRICE CODE

17. SECURITY CLASSIFICATION OF REPORT	18. SECURITY CLASSIFICATION OF THIS PAGE	19. SECURITY CLASSIFICATION OF ABSTRACT	20. LIMITATION OF ABSTRACT
UNCLASSIFIED	UNCLASSIFIED	UNCLASSIFIED	UL

I. INTRODUCTION

Electrically and/or physically small antennas are often required by missile systems because of limited space requirements or reduction in radar cross section. For some systems, even at UHF and VHF frequencies, the antenna can be isolated as the single most heavy and bulky component (Reference 1). Reduction in size presents problems for the system designer due to the performance penalties in bandwidth and efficiency that arise. These performance penalties must be absorbed into the overall system performance resulting in poor reception in low signal regions. Matching techniques can be used to boost antenna performance but a reduction in total efficiency is still incurred.

Several methods to counteract the above problems have been considered. For small antennas with radiation resistances lower than the ohmic resistances of their radiating elements and which include feed and matching networks, higher efficiencies have been measured when all components are composed of high temperature superconducting (HTS) materials (References 2 through 5). However, this replacement of normal conductors with HTS components can only partially compensate for the drop in efficiency upon size reduction. Thus it is advantageous to obtain as large an efficiency as possible from a given antenna by other means first.

One such method has been investigated for some years by D. M. Grimes (References 6 through 11). This method consists of using judicious combinations of electric and magnetic multipole sources to attempt to exceed the small antenna limitations derived by Chu (Reference 12), Harrington (References 13 and 14), and Wheeler (References 15 and 16). Since most of Grimes' analyses on this subject are very general, in this report we investigate the most simple case of the above, i.e., an electrically small colocated array composed of an electric dipole and a magnetic loop (modelled as an orthogonal equivalent magnetic dipole). We have found that, even for this simple case, the individual electric and magnetic field components combine in such a way that the interaction term involving the currents on both array elements disappears from the complex power. This allows the reactive part of the complex power to be set to zero when appropriate amplitude and phase ratios between the dipole current and the loop current are used. Inputting the derived currents into the numerical code, NEC3D, we find that the radiated power is significantly increased over the corresponding power resulting from an electric dipole or a magnetic loop alone. We have determined that the loop current must be driven in phase quadrature to the dipole current in order for this increased radiated power effect to be seen. If the currents are simply in phase, the array radiates exactly as if each element stood alone. Similarly the directivity of the array is the same as that of a dipole alone or a loop alone if the respective currents are in phase, but the directivity of the array is doubled if the respective currents are in phase quadrature.

In Section II, we determine the total field components of the electric dipole, magnetic loop array in simplified form, i.e., without resorting to Hankel and Legendre functions. In Section III we compute the radial part of the complex Poynting vector, the radial complex power, and the current amplitude ratio which gives zero reactive power. In

Section IV we derive the radiation intensity and directivity of the array for two cases: (1) when the dipole and loop currents are in phase and (2) when they are in phase quadrature. The NEC3D numerical results are presented in Section V, a general discussion on antenna element coupling is presented in Section VI, and conclusions appear in Section VII.

II. THEORY

Consider the geometry of Figure 1. We assume that the antenna consists of two elements, an electric dipole oriented along the $\hat{z}$ axis and a magnetic loop oriented in the same plane, the yz plane. The loop and dipole are colocated and nontouching. The dipole runs from - $\ell/2$ to $\ell/2$ along $\hat{z}$ with a total length ℓ and a current I_d. The loop has a radius, "a," and a current I_ℓ. We assume that both elements are electrically very small and thus considered to be infinitesimal ($\leq\lambda/50$) for analysis purposes.

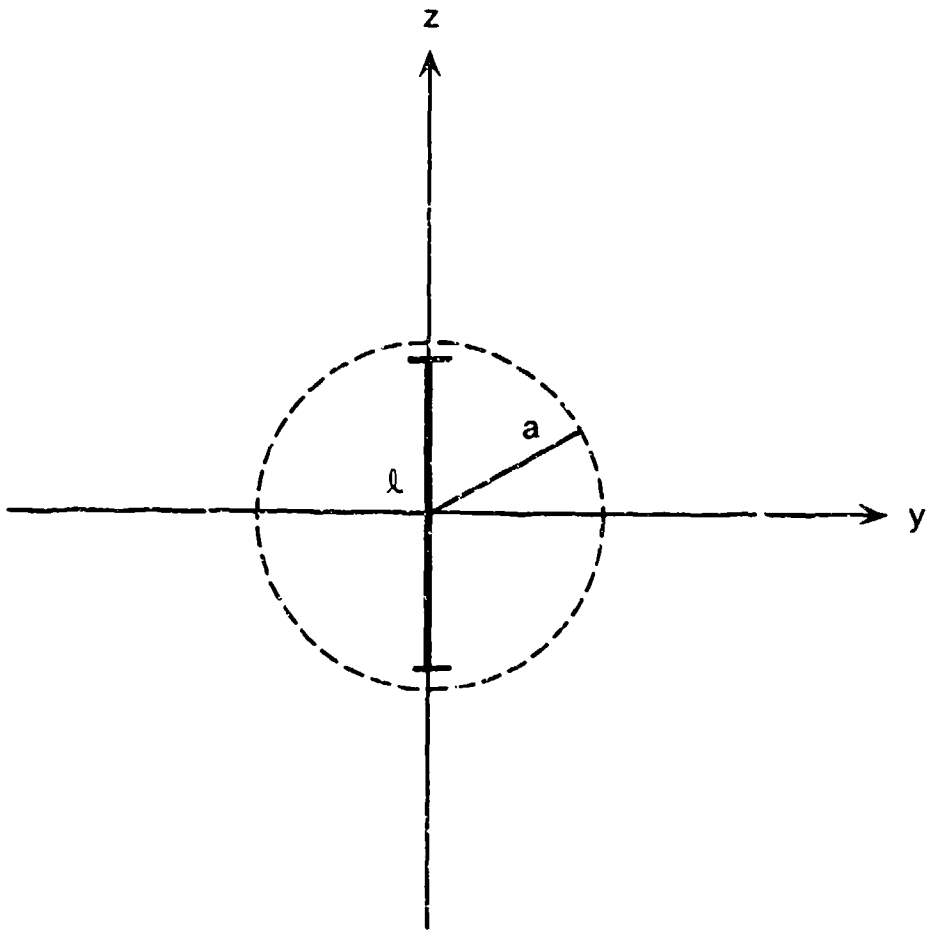

FIGURE 1. Antenna Geometry.

Since the dipole is oriented along the $\hat{z}$ axis, its electromagnetic field components in spherical coordinates (for a constant current) are (Reference 17):

$$H_r^{(1)} = H_\theta^{(1)} = E_\phi^{(1)} = 0 \quad , \tag{1a}$$

$$H_\phi^{(1)} = \frac{ikI_d \ell \sin\theta}{4\pi r}\left(1+\frac{1}{ikr}\right)e^{-ikr} \quad , \tag{1b}$$

$$E_r^{(1)} = \frac{\eta I_d \ell \cos\vartheta}{2\pi r^2}\left(1+\frac{1}{ikr}\right)e^{-ikr} \quad , \tag{1c}$$

$$E_\theta^{(1)} = \frac{i\eta k I_d \ell \sin\theta}{4\pi r}\left[1+\frac{1}{ikr}-\frac{1}{(kr)^2}\right]e^{-ikr} \quad , \tag{1d}$$

where $k = \frac{2\pi}{\lambda}$, $\eta = \sqrt{\frac{\mu}{\varepsilon}}$, and the superscript 1 indicates that these are dipole fields. Now we must put the loop into the same coordinate frame. Standard analyses of loop antennas place them in the xy plane with $\hat{z}$ normal to the loop. In our case the loop is located in the yz plane with $\hat{x}$ as its normal. We invoke the usual equivalency between an infinitesimal loop of radius a, current I_ℓ, and an infinitesimal magnetic dipole of length ℓ_m, current I_m which (in our case) runs along the $\hat{x}$ axis. Thus (Reference 17)

$$I_m \ell_m = i\left(\pi a^2\right)\omega\mu I_\ell = i\left(\pi a^2\right)k\eta I_\ell \quad . \tag{2}$$

An equivalent magnetic dipole along the $\hat{x}$ axis has

$$\vec{A} = 0$$

$$\vec{F}(x,y,z) = \frac{\varepsilon}{4\pi}\int_c \vec{I}_m(x',y',z')\frac{e^{-ikR}}{R}d\ell' \tag{3}$$

where $\vec{A}$ and $\vec{F}$ are the usual magnetic and electric vector potentials, respectively. Using $\vec{I}_m = I_m \hat{x}$ where I_m is assumed to be constant and assuming that $R \approx r$, the electric vector potential becomes

$$\vec{F} = \hat{x} \frac{\varepsilon I_m \ell_m}{4\pi r} e^{-ikr} \quad . \tag{4}$$

Using the transformation between Cartesian and spherical coordinates,

$$\begin{pmatrix} F_r \\ F_\theta \\ F_\phi \end{pmatrix} = \begin{pmatrix} \sin\theta\cos\phi & \sin\theta\sin\phi & \cos\theta \\ \cos\theta\cos\phi & \cos\theta\sin\phi & -\sin\theta \\ -\sin\phi & \cos\phi & 0 \end{pmatrix} \begin{pmatrix} F_x \\ 0 \\ 0 \end{pmatrix} \quad , \tag{5}$$

we obtain

$$F_r = \frac{\varepsilon I_m \ell_m}{4\pi r} \sin\theta\cos\phi\, e^{-ikr} \tag{6a}$$

$$F_\theta = \frac{\varepsilon I_m \ell_m}{4\pi r} \cos\theta\cos\phi\, e^{-ikr} \tag{6b}$$

$$F_\phi = \frac{-\varepsilon I_m \ell_m}{4\pi r} \sin\phi\, e^{-ikr} \quad . \tag{6c}$$

The electric field components of the loop are given by

$$\vec{E} = -\frac{1}{\varepsilon} \nabla x \vec{F} \tag{7}$$

or

$$E_r^{(2)} = 0 \tag{8a}$$

$$E_\theta^{(2)} = \frac{ikI_m\ell_m}{4\pi r}\sin\phi\left(1+\frac{1}{ikr}\right)e^{-ikr} \quad , \tag{8b}$$

$$E_\phi^{(2)} = \frac{ikI_m\ell_m}{4\pi r}\cos\theta\cos\phi\left(1+\frac{1}{ikr}\right)e^{-ikr} \tag{8c}$$

where the superscript 2 indicates that these are loop fields.

Using

$$\vec{H} = \frac{1}{i\omega\mu}\nabla x\vec{E} \quad , \tag{9}$$

the magnetic field components are

$$H_r^{(2)} = \frac{I_m\ell_m}{\eta 2\pi r^2}\sin\theta\cos\phi\left(1+\frac{1}{ikr}\right)e^{-ikr} \quad , \tag{10a}$$

$$H_\theta^{(2)} = \frac{-ikI_m\ell_m}{\eta 4\pi r}\cos\theta\cos\phi\left[1+\frac{1}{ikr}-\frac{1}{(kr)^2}\right]e^{-ikr} \tag{10b}$$

$$H_\phi^{(2)} = \frac{ikI_m\ell_m}{\eta 4\pi r}\sin\phi\left[1+\frac{1}{ikr}-\frac{1}{(kr)^2}\right]e^{-ikr} \quad . \tag{10c}$$

Thus the total field components of the dipole and the loop should be simply a superposition of the field components from each element alone. Using

$$\vec{E} = \vec{E}^{(1)} + \vec{E}^{(2)} \quad ; \quad \vec{H} = \vec{H}^{(1)} + \vec{H}^{(2)} \quad , \tag{11}$$

the total field components are

$$E_r = \frac{\eta I_d \ell}{2\pi r^2}\cos\theta\left(1+\frac{1}{ikr}\right)e^{-ikr} \tag{12a}$$

$$E_\theta = \frac{i\eta k I_d \ell}{4\pi r}\sin\theta\left[1+\frac{1}{ikr}-\frac{1}{(kr)^2}\right]e^{-ikr} + \frac{ikI_m\ell_m}{4\pi r}\sin\phi\left(1+\frac{1}{ikr}\right)e^{-ikr} \tag{12b}$$

$$E_\phi = \frac{ikI_m\ell_m}{4\pi r}\cos\theta\cos\phi\left(1+\frac{1}{ikr}\right)e^{-ikr} \tag{12c}$$

$$H_r = \frac{I_m\ell_m}{\eta 2\pi r^2}\sin\theta\cos\phi\left(1+\frac{1}{ikr}\right)e^{-ikr} \tag{12d}$$

$$H_\theta = \frac{-ikI_m\ell_m}{\eta 4\pi r}\cos\theta\cos\phi\left[1+\frac{1}{ikr}-\frac{1}{(kr)^2}\right]e^{-ikr} \tag{12e}$$

$$H_\phi = \frac{ikI_d\ell}{4\pi r}\sin\theta\left(1+\frac{1}{ikr}\right)e^{-ikr} + \frac{ikI_m\ell_m}{\eta 4\pi r}\sin\phi\left[1+\frac{1}{ikr}-\frac{1}{(kr)^2}\right]e^{-ikr} \tag{12f}$$

Equations 12 are a superposition of a TM (to $\hat{r}$) mode from the dipole and a TE (to $\hat{r}$) mode from the loop. The field components from the dipole have no ϕ dependence, while those from the loop have both θ and ϕ dependence in general (although $E_\theta^{(2)}$ and $H_\phi^{(2)}$ are not functions of θ) Of the total field components given by Equations 12, none are zero, but only two, E_θ and H_ϕ, contain contributions from both the dipole and the loop.

III. THE RADIAL PART OF THE COMPLEX POYNTING VECTOR AND COMPLEX POWER

The usual complex Poynting vector is defined to be (References 17 and 18)

$$\vec{S_c} = \frac{1}{2}\left(\vec{E}\times\vec{H}^*\right) \quad , \tag{13}$$

or in component form

$$S_{c_r} = \frac{1}{2}\left(E_\theta H_\phi^* - E_\phi H_\theta^*\right) \quad , \tag{14a}$$

$$S_{c_\theta} = \frac{1}{2}\left(E_\phi H_r^* - E_r H_\phi^*\right) \quad , \tag{14b}$$

$$S_{c_\phi} = \frac{1}{2}\left(E_r H_\theta^* - E_\theta H_r^*\right) \quad . \tag{14c}$$

For now, we will consider only the radial part of the complex Poynting vector given by Equation 14a. Using Equations 12 and after some algebra, Equation 14a becomes

$$\begin{aligned} S_{c_r} = \frac{1}{2}\Bigg\{ & \frac{\eta k^2 |I_d \ell|^2}{(4\pi r)^2} \sin^2\theta \left[1 - \frac{i}{(kr)^3}\right] \\ & + \frac{k^2 I_d \ell (I_m \ell_m)^*}{(4\pi r)^2} \sin\theta \sin\phi \left[1 - \frac{1}{(kr)^2} + \frac{1}{(kr)^4}\right] \\ & + \frac{k^2 (I_d \ell)^* I_m \ell_m}{(4\pi r)^2} \sin\theta \sin\phi \left[1 + \frac{1}{(kr)^2}\right] \\ & + \frac{k^2 |I_m \ell_m|^2}{\eta (4\pi r)^2} \left[\sin^2\phi + \cos^2\theta \cos^2\phi\right] \left[1 + \frac{i}{(kr)^3}\right] \Bigg\} \quad . \end{aligned} \tag{15}$$

To obtain complex power travelling in the radial direction, we integrate the radial part of the complex Poynting vector over a sphere of radius r. So

$$P = \oiint \vec{S_c} \cdot d\vec{s} \tag{16}$$

$$= \int_0^{2\pi} \int_0^{\pi} \left[S_{c_r} \hat{r} + S_{c_\theta} \hat{\theta} + S_{c_\phi} \hat{\phi} \right] \cdot \left[r^2 \sin\theta \, d\theta d\phi \, \hat{r} \right] \tag{17}$$

or

$$P = r^2 \int_0^{2\pi} \int_0^{\pi} S_{c_r} \sin\theta \, d\theta d\phi \tag{18}$$

with S_{cr} given by Equation 15. Considering the four terms in Equation 15 and since we only have to integrate over the angular dependence, the first term in Equation 15 leads to an integral of the form

$$I_1 = \int_0^{2\pi} \int_0^{\pi} \sin^3\theta \, d\theta d\phi \quad , \tag{19}$$

the second and third terms in Equation 15 lead to

$$I_2 = \int_0^{2\pi} \int_0^{\pi} \sin^2\theta \sin\phi \, d\theta d\phi \quad , \tag{20}$$

and the fourth term in Equation 15 leads to

$$I_3 = \int_0^{2\pi} \int_0^{\pi} \left(\sin^2\phi + \cos^2\theta \cos^2\phi \right) \sin\theta \, d\theta d\phi \quad . \tag{21}$$

Performing the integrations in Equations 19 through 21, $I_1 = \frac{8\pi}{3}$, $I_2 = 0$, $I_3 = \frac{8\pi}{3}$. Thus the complex radial power becomes

$$P = \frac{8\pi}{6}\left\{\frac{\eta k^2 |I_d \ell|^2}{(4\pi)^2}\left[1 - \frac{i}{(kr)^3}\right] + \frac{k^2 |I_m \ell_m|^2}{\eta (4\pi)^2}\left[1 + \frac{i}{(kr)^3}\right]\right\} \quad . \tag{22}$$

Because the second integration, given by Equation 20 vanishes, the interaction terms between the dipole and the loop disappear from the radial complex power. These cross terms are still present in the complex Poynting vector.

Splitting Equation 22 into real and imaginary parts,

$$\mathrm{Re}(P) = \frac{\eta\pi}{3\lambda^2}\left(|I_d \ell|^2 + \frac{|I_m \ell_m|^2}{\eta^2}\right) \tag{23a}$$

and

$$\mathrm{Im}(P) = \frac{\eta\pi}{3\lambda^2}\left(-|I_d \ell|^2 + \frac{|I_m \ell_m|^2}{\eta^2}\right)\frac{1}{(kr)^3} \quad . \tag{23b}$$

If we interpret Equation 23a as the radial radiated power and Equation 23b as the radial reactive or stored power, then

$$P_{rad} = \frac{\eta\pi}{3\lambda^2}\left(|I_d \ell|^2 + \frac{|I_m \ell_m|^2}{\eta^2}\right) \tag{24a}$$

and

$$2\omega\left(\tilde{W}_m - \tilde{W}_e\right) = \frac{\eta\pi}{3\lambda^2}\left(\frac{|I_m \ell_m|^2}{\eta^2} - |I_d \ell|^2\right)\frac{1}{(kr)^3} \tag{24b}$$

where P_{rad} is the time-averaged radiated power, ω is the frequency, and $\tilde{W}_m$ and $\tilde{W}_e$ are the time-averaged magnetic and electric radial energies, respectively.

Due to the disappearance of the interaction terms between the loop and the dipole in the complex radial power, we can set the reactive or stored power to zero by insisting that

$$|I_d \ell|^2 = \frac{|I_m \ell_{in}|^2}{\eta^2} \quad . \tag{25}$$

Using Equation 2, the proper current amplitude ratio for zero reactive power is

$$\left|\frac{I_\ell}{I_d}\right|^2 = \frac{\left(\frac{\ell}{\lambda}\right)^2}{\left(2\pi^2\right)^2\left(\frac{a}{\lambda}\right)^4} \quad . \tag{26}$$

However, Equation 26 does not tell us about the relative phases of the dipole and loop currents. We will discuss this issue in Section IV.

IV. RADIATION INTENSITY, DIRECTIVITY, AND RELATIVE CURRENT PHASES

From the total field components in Equations 12, in the far-field these components become

$$E_r \approx H_r \approx 0 \quad , \tag{27a}$$

$$E_\theta \approx \frac{ik\eta e^{-ikr}}{4\pi r}\left(\eta I_d \ell \sin\theta + iAkI_\ell \sin\phi\right) \quad , \tag{27b}$$

$$E_\phi \approx \frac{-k^2 A\eta I_\ell e^{-ikr}}{4\pi r}\cos\theta\cos\phi \tag{27c}$$

with

$$H_\theta = -\eta E_\phi \quad ; \quad H_\phi = \eta E_\theta \tag{28}$$

and $A = \pi a^2$, the loop area.

The radiation intensities, U_θ and U_ϕ, are

$$U_\theta = \frac{r^2|E_\theta|^2}{2\eta} \quad ; \quad U_\phi = \frac{r^2|E_\phi|^2}{2\eta} \tag{29}$$

and we will consider two separate cases based on the phase relationship between the loop and dipole currents.

Case 1. Let I_d be pure real and I_ℓ be pure real. Then since they are in phase

$$U_\theta = \frac{\eta}{8}\left[\left(\frac{\ell}{\lambda}\right)^2 \sin^2\theta + \left(2\pi^2\right)^2\left(\frac{a}{\lambda}\right)^4\left(\frac{I_\ell}{I_d}\right)^2 \sin^2\phi\right] \tag{30a}$$

and

$$U_\phi = \frac{\eta\pi^4\left(\frac{a}{\lambda}\right)^4}{2}\left(\frac{I_\ell}{I_d}\right)^2 \cos^2\theta\cos^2\phi \tag{30b}$$

and the total intensity is

$$U = \frac{\eta}{8}\left[\left(\frac{\ell}{\lambda}\right)^2 \sin^2\theta + \left(2\pi^2\right)^2\left(\frac{a}{\lambda}\right)^4\left(\frac{I_\ell}{I_d}\right)^2\left(\sin^2\phi + \cos^2\theta\cos^2\phi\right)\right] \quad . \tag{31}$$

Since the radiated power is given by Equation 24a, we can obtain both the directive gain from

$$D_g = \frac{4\pi U}{P_{rad}} \tag{32}$$

and the directivity from

$$D_o = \frac{4\pi U_{max}}{P_{rad}} \quad . \tag{33}$$

The directive gain is plotted for $\phi = \left(\frac{\pi}{2}\right)$ in Figure 2 with $\left(\frac{I_\ell}{I_d}\right)$ as a parameter for I_ℓ and I_d in phase. The maximum directivity of this antenna (when the currents are in phase) is 3/2 (1.76 dB), exactly the same value as the directivity of the small dipole alone, or the small loop alone (Reference 17).

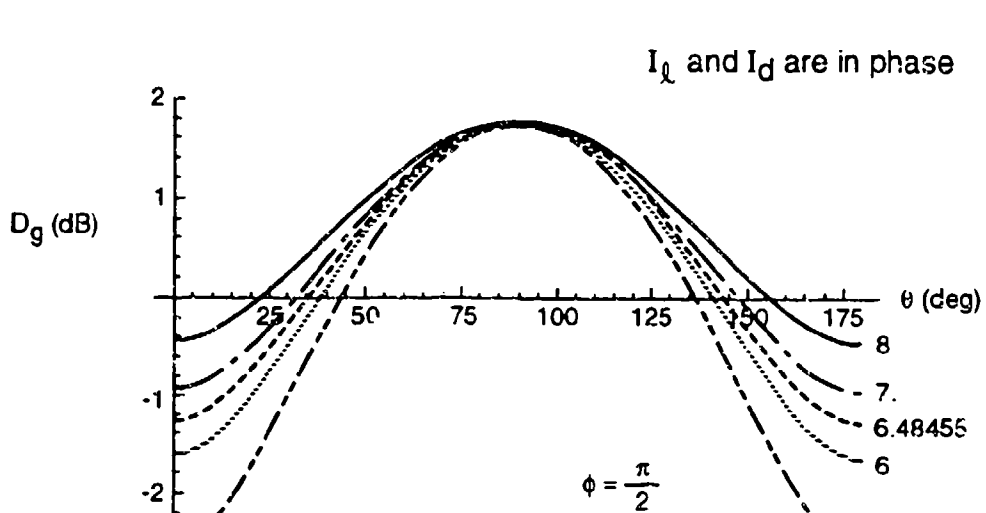

FIGURE 2. Directive Gain When Array Element Currents are in Phase.

Case 2. Let I_d be real and $I_\ell = -iI_\ell'$ where I_ℓ' is real. The two currents are now 90 degrees out of phase, or in quadrature. Now

$$E_\theta \approx \frac{ik\eta e^{-ikr}}{4\pi r}\left(I_d \ell \sin\theta + AkI_\ell' \sin\phi\right) \tag{34a}$$

and

$$E_\phi \approx \frac{ik^2 A\eta I_\ell' e^{-ikr}}{4\pi r} \cos\theta \cos\phi \quad . \tag{34b}$$

Thus the radiation intensities for this case are

$$U_\theta = \frac{\eta}{8}\left[\left(\frac{\ell}{\lambda}\right)^2 \sin^2\theta + 4\pi^2\left(\frac{\ell}{\lambda}\right)\left(\frac{a}{\lambda}\right)^2\left(\frac{I'_\ell}{I_d}\right)\sin\theta\sin\phi\right. \tag{35a}$$

$$\left. +4\pi^4\left(\frac{a}{\lambda}\right)^4\left(\frac{I'_\ell}{I_d}\right)^2\left(\sin^2\phi + \cos^2\theta\cos^2\phi\right)\right]$$

and

$$U_\phi = \frac{\eta\pi^4\left(\frac{a}{\lambda}\right)^4}{2}\left(\frac{I'_\ell}{I_d}\right)^2\cos^2\theta\cos^2\phi \quad . \tag{35b}$$

Immediately we see that Equation 35a contains extra terms when compared with Equation 30a. U_ϕ as given by Equations 30b and 35b is the same for both cases. When $\phi = 0$, Equations 30a and 35a are identical for the same $\left(\frac{I_\ell'}{I_d}\right)$. When $\phi = \frac{\pi}{2}$, Equation 35a is larger than Equation 30a (see Figure 3). Where the directive gain is computed using Equation 35, the amplitude as well as the shape of the curves are quite different from the in phase case. The maximum directivity is 3(4.77 dB) in this case when $\left|\frac{I_\ell'}{I_d}\right|$ is given by Equation 26. Thus the antenna directivity for currents in quadrature is twice as much as the directivity resulting when the currents are in phase.

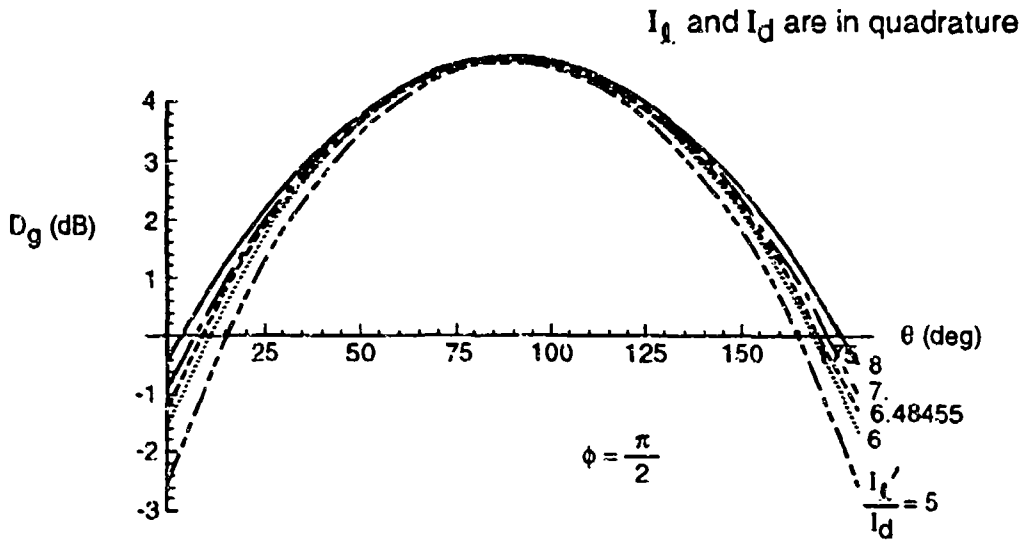

FIGURE 3. Directive Gain When Array Element Currents are in Quadrature.

V. MUTUAL AND DRIVING POINT IMPEDANCES USING NEC3D

This section describes the approach used in modelling the colocated magnetic loop and electric dipole array shown in Figure 1 (also see Reference 19). The modelling approach can be summarized by the following steps:

(1) Find the array Y-matrix using Method of Moments (MOM)
(2) Find the array Z-matrix (by inversion of Y-matrix)
(3) Determine desired current excitations for both loop and dipole
(4) Determine active port impedances for both loop and dipole from:

$$za_i = z_{i1} \cdot \frac{I_1}{I_i} + z_{i2} \cdot \frac{I_2}{I_i} + \cdots + z_{ii} + \cdots + z_{in} \cdot \frac{I_n}{I_i} \tag{36}$$

where

Za_i is the active impedance at the ith port
Z_{ij} is the i,jth element of the Z-matrix
I_i is the current at the ith port

The remainder of this section will discuss each of the above steps in more detail and present results for the colocated array.

FINDING THE Y-MATRIX USING MOM

In the MOM approach the antenna array geometry is first defined by wire segments as shown in Figure 4. The electrically small loop to be analyzed has been assumed to be square with side length of 0.025 λ. Each side of the loop is subdivided into five segments. The loop is centered about the origin and is located in the yz plane. The dipole is also centered about the origin and is located along the z-axis with total length of 0.020 λ. The dipole is also divided into five segments. For this example, the radius of the wire was chosen as 0.001 λ. The total length of the dipole was adjusted to be 80% of the loop side length to avoid close proximity of the ends of the dipole with segments in the loop. The effects of varying the relative dipole length have not been investigated but changes are not expected to change the basic operating principles of the colocated array.

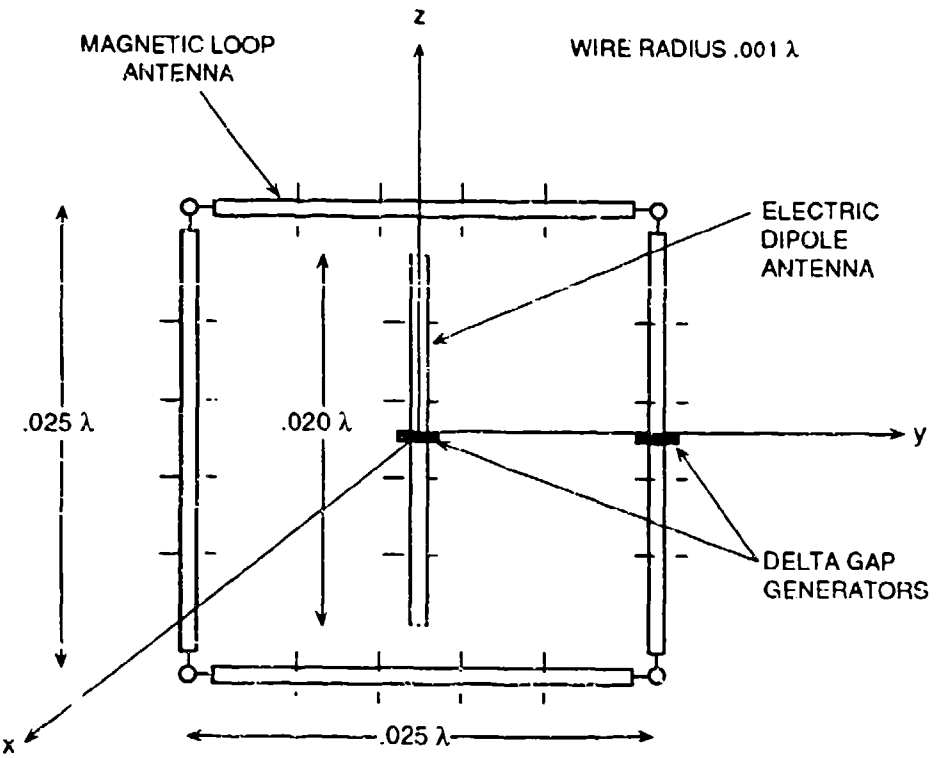

FIGURE 4. Colocated Antenna Geometry for Method of Moments Analysis.

In MOM the array is excited by inserting delta gap voltage generators of specified magnitude and phase at the center of a wire segment. The currents are then determined in each of the segments according to the MOM procedure. As will be shown below the MOM approach lends itself to direct computation of the two port Y matrix of the array. The Y matrix of a two port is described in terms of the terminal voltages and currents by:

$$I_1 = Y_{11} V_1 + Y_{12} V_2$$

$$I_2 = Y_{21} V_1 + Y_{22} V_2 \quad . \tag{37}$$

Notice that if V_1 is set to 1 volt, and V_2 is set to zero, Y_{11} is identically equal to the current I_1 and Y_{21} is equal to I_2. Similarly, if V_1 is set to zero and V_2 is set to 1 volt, then Y_{12} is equal to the current I_1 and Y_{22} is equal to I_2. In this fashion the Y matrix can be directly computed from the MOM derived currents since the delta gap voltage can be set to 1 volt and the voltage set to zero by replacing the delta gap generator by a wire segment (i.e. removing the delta gap generator). The Y matrix computed for the example in Figure 4 (with lossless conductors) at a frequency of 500 MHz is:

$$Y = \begin{pmatrix} 1.1293 \cdot 10^{-9} + 3.4111 \cdot 10^{-4} i & 7.4836 \cdot 10^{-9} - 5.8541 \cdot 10^{-5} i \\ 7.7687 \cdot 10^{-9} - 5.5983 \cdot 10^{-5} i & 1.4187 \cdot 10^{-6} - 0.01039 i \end{pmatrix} \tag{38}$$

The above values were computed using Numerical Electromagnetics Code (NEC), version NEC3D run on a Macintosh IIsi. NEC was developed at the Lawrence Livermore Laboratory under the sponsorship of the Naval Ocean Systems Center and the Air Force Weapons Laboratory.

ARRAY Z MATRIX

The Y matrix can be inverted to give the Z matrix

$$Z = \begin{pmatrix} 0.00934 - 2.9289 \cdot 10^{3} i & 9.13542 \cdot 10^{-5} + 16.50405 i \\ -8.52033 \cdot 10^{-5} + 15.78289 i & 0.01314 + 96.16672 i \end{pmatrix} \quad . \tag{39}$$

Z_{11} corresponds to the self impedance of the dipole and Z_{22} is the self impedance of the loop. Since in this example conductors are assumed lossless, R_{11} and R_{22} represent the radiation resistances of the dipole and loop, respectively, and since both loop and dipole are electrically small, the radiation resistance of each isolated antenna is correspondingly very small. One of the prime motivations for this hybrid mode array is to significantly increase the radiation resistance of the electrically small antennas without increasing their physical size.

COMPUTING CURRENT EXCITATIONS OF HYBRID MODE ANTENNA

Using Equation 26 from Section III that specifies the proper current ratio for zero reactive power and rewriting the denominator in terms of the area of the loop, A, gives

$$\frac{I_\ell}{I_d} = \frac{i \cdot \frac{\ell}{\lambda}}{2 \cdot \pi \cdot \frac{A}{\lambda^2}} \quad . \tag{40}$$

For a square loop with side length S the proper ratio is

$$\frac{I_\ell}{I_d} = \frac{i \cdot \frac{\ell}{\lambda}}{2 \cdot \pi \cdot \left(\frac{S}{\lambda}\right)^2} \quad , \tag{41}$$

for ℓ/λ = 0.020, S/λ = 0.025, and I_ℓ/I_d = i 5.093. Thus, the current in the loop is approximately five times that in the dipole, and the currents are in quadrature.

ACTIVE IMPEDANCES OF HYBRID MODE ANTENNA

The active impedances are computed from Equation 36 and listed in Table 1 for the relative current excitations shown.

TABLE 1.

I_{dipole}	I_{loop}	Za_{dipole}	Za_{loop}
$1 \angle 0°$	5.093	0.0098 - i2844.8	0.01313 + i99.266
$1 \angle 90°$	5.093	84.064 -i2928.9	-3.086 + i96.17
$1 \angle 180°$	5.093	0.0089 - i3013.0	0.01316 + i93.068
$1 \angle 270°$	5.093	-84.045 - i2928.9	3.112 + i96.167

It is important to note that when the currents are in quadrature the radiation resistance of both the loop and dipole is significantly increased. If the currents are not in quadrature the radiation resistance is approximately that of the isolated element. Furthermore, with the currents in quadrature the radiation resistance of one element is positive and the radiation resistance of the other element is negative. The physical interpretation of a negative radiation resistance is that rather than radiating power (as would be the case for a positive radiation resistance), an antenna with a negative radiation resistance is receiving power and delivering it to the load connected to the port. The significance of colocation and quadrature currents in the large increase in radiation resistance can be seen in the expression for the active impedances of a two port colocated antenna array,

$$Za_1 = Z_{11} + Z_{12} \cdot \frac{I_2}{I_1}$$

$$Za_2 = Z_{21} \cdot \frac{I_1}{I_2} + Z_{22} \quad . \tag{42}$$

From Equation 39 the mutual coupling (Z_{12} and Z_{21}) for colocated antennas is observed to have a large reactive component. As the separation between antennas is increased the magnitude of the mutual coupling also decreases. The large reactive component of the mutual coupling combined with the currents in quadrature results in a significant real resistive component in the active impedance compared to the small radiation resistance due to the self impedance of electrically small antennas.

SENSITIVITY TO MAGNITUDE AND PHASE PERTURBATIONS

Table 2 lists computed active impedances for current excitations that deviate from the specified current ratio of Equation 41.

TABLE 2.

I_{dipole} , I_{loop}	Za_{dipole}	Za_{loop}	P_{dipole} , P_{loop}
$1 \angle 90°$, 6.000	99.035 - i2928.9	-2.617 + i96.17	49.52 , -47.11
$1 \angle 90°$, 5.093	84.064 - i2928.9	-3.086 + i96.17	42.03 , -40.02
$1 \angle 90°$, 5.000	82.531 - i2928.9	-3.144 + i96.17	41.27 , -39.29
$1 \angle 90°$, 4.000	66.027 - i2928.9	-3.933 + i96.17	33.01 , -31.46
$1 \angle 85°$, 5.093	83.746 - i2921.6	-3.074 + i96.44	41.87 , -39.87
$1 \angle 45°$, 5.093	59.446 - i2869.5	-2.178 + i98.36	29.72 , -28.25
$1 \angle 135°$, 5.093	59.446 - i2988.4	-2.178 + i93.98	29.72 , -28.24

Thus, it appears that the colocated antenna is relatively insensitive to small perturbations in the magnitude and phase of the excitation currents. The powers listed for the dipole and loop are the radiated power from the dipole (positive) and the power received by the loop (negative), respectively. The total radiated power of the array is the algebraic sum. As the magnitude of the current in the loop is decreased the total radiated power also decreases.

VI. GENERAL DISCUSSION ON ANTENNA ELEMENT COUPLING

In antenna arrays the relative input currents to the individual antenna elements are specified as to their relative magnitudes and phases in order to obtain the desired gain, pattern, radiation direction, etc.

With close packed arrays, (and a colocated loop and dipole is certainly an example) where the coupling between the elements cannot be ignored, a serious efficiency problem can arise.

Consider our two-element array as a two port as in Figure 5a, with impedance matrix (Z) and scattering matrix (S). It follows that the active input impedances looking into ports (or antenna elements) one and two are:

$$Z_1 = Z_{11} + Z_{12}\frac{I_2}{I_1} \tag{43a}$$

$$Z_2 = Z_{22} + Z_{12}\frac{I_1}{I_2} \quad . \tag{43b}$$

Since the Z_{ij} are fixed by the geometry of the situation and I_2 and I_1 are fixed by the antenna performance requirements, Z_1 and Z_2 are fixed impedances with specific numerical values.

The active impedances, Z_1 and Z_2, represent the impedances that must be matched into in order to increase the system efficiency and radiate as much of the available power as possible. The matching problem reduces to Figure 5b with some provisos that we will note as we proceed.

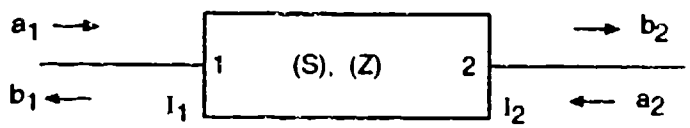

FIGURE 5(a). Two-Element Array as a Two Port.

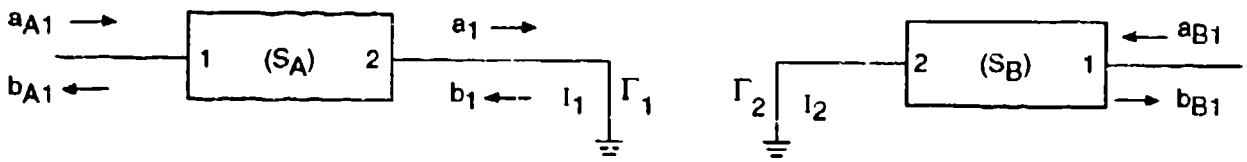

FIGURE 5(b). Reduction of Two Port Matching Problem.

The active reflection coefficients, Γ_1 and Γ_2, are given by

$$\Gamma_i = \frac{Z_i - Z_0}{Z_i + Z_0} \quad ; \quad i = 1,2 \tag{44}$$

while (S_A) and (S_B) represent matching networks with the goal of reducing the reflected waves b_{A1} and b_{B1} to zero while simultaneously not introducing loss in the matching networks themselves.

For a lossless matching network, the condition for zero reflection is given by

$$S_{A22} = \Gamma_1^* \quad ; \quad S_{B22} = \Gamma_2^* \quad . \tag{45}$$

The other scattering coefficients of the matching networks can then be found by imposing the usual unitary condition

$$(S)\left(S^T\right)^* = (U) \tag{46}$$

on the matching networks.

It should be noted that merely attaching the matching networks thus designed to the antenna array input ports will not ensure proper performance of the antenna array. The drive levels a_{A1} and a_{B1} into the matching networks must be of the proper relative magnitude and phase to provide the correct relative currents I_1 and I_2. The relations between a_{B1} and the S_{Aij} and current I_1 are readily found as are the relations between a_{B1} and the S_{Bij} and current I_2.

The drive levels a_{A1} and a_{B1} would generally be supplied from an uneven power divider designed to give the proper complex ratio a_{A1}/a_{B1} with the system looking like Figure 6.

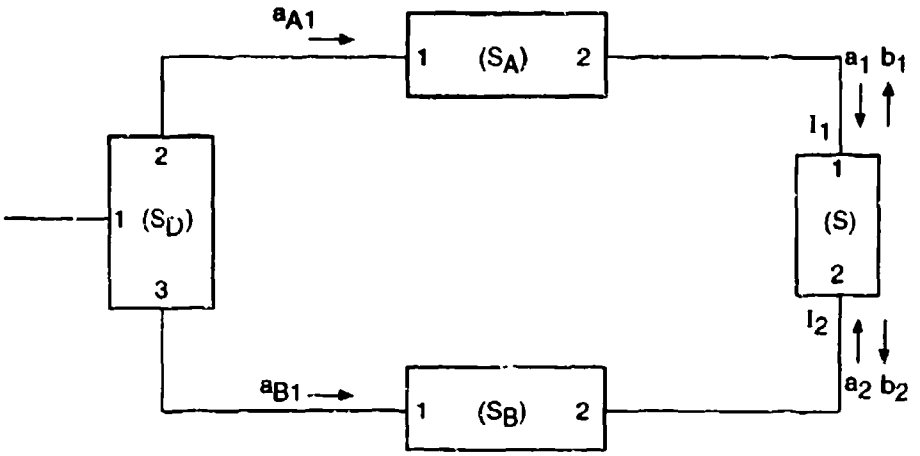

FIGURE 6. Two-Element Array With Matching Networks.

As long as Equation 45 can be satisfied, there is no reason, in principal, why lossless matching networks and power dividers cannot be designed and built to a good degree of approximation. If the coupling between antenna elements is sufficiently strong, and the currents, I_1 and I_2, have sufficiently different magnitudes and phases, the real part of Z_1 or Z_2 (but not both due to the conservation of energy) can be negative. When that is the case, the magnitude of the active reflection coefficient is greater than unity and cannot be matched using a lossless network.

For the electric dipole and the loop with I_1 and I_2 set to "zero out" the imaginary part of the complex Poynting vector, this is precisely the case as shown in Table 1. The mechanism by which this occurs is readily seen by rewriting Equations 43a and 43b:

$$Z_1 = R_1 + iX_1 = R_{11} + \left|\frac{I_2}{I_1}\right|(R_{12}\cos\Delta\phi - X_{12}\sin\Delta\phi) \tag{47a}$$

$$+ i\left[X_{11} + \left|\frac{I_2}{I_1}\right|(R_{12}\sin\Delta\phi + X_{12}\cos\Delta\phi)\right] ,$$

$$Z_2 = R_2 + iX_2 = R_{22} + \left|\frac{I_1}{I_2}\right|(R_{12}\cos\Delta\phi + X_{12}\sin\Delta\phi) \tag{47b}$$

$$+ i\left[X_{22} + \left|\frac{I_1}{I_2}\right|(X_{12}\cos\Delta\phi - R_{12}\sin\Delta\phi)\right]$$

where $\Delta\phi$ is the phase shift between I_1 and I_2. If $|I_2|>>|I_1|$, for example, and R_{12} is small, and $\Delta\phi = \pi/2$, it is easily seen that R_1 may very well be negative, while R_2 is positive. (R_{11} and R_{22} in the impedance matrix must be positive without the presence of active devices.)

If a negative R_1 is the case then the matching problem leads to Figure 7, where Γ_A is chosen to give the proper current at port 1 of our antenna array.

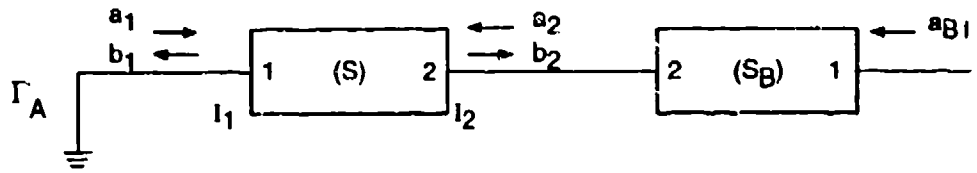

FIGURE 7. The Matching Problem When R_1 is Negative.

Figure 8 is equivalent to Figure 7 and maintaining the proper value of I_1 must be done by setting Γ_A equal to the reciprocal of Γ_1.

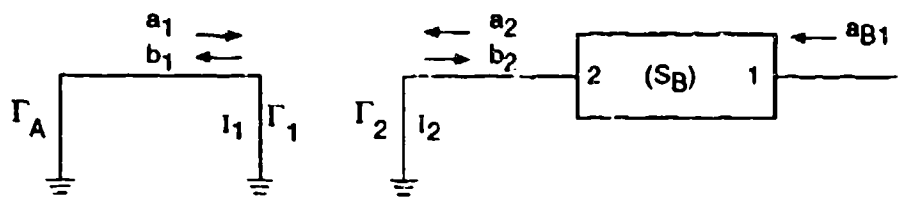

FIGURE 8. Equivalent System to Figure 7.

$$I_1 = \frac{1}{Z_0}(a_1 - b_1) = \frac{a_1}{Z_0}(1 - \Gamma_1) = \frac{a_1}{Z_0}\left(1 - \frac{1}{\Gamma_A}\right) \quad . \tag{48}$$

Solving (48) for Γ_A gives

$$\Gamma_A = \frac{1}{\Gamma_1} \quad . \tag{49}$$

$$Z_A = |R_1| - iX_1 \tag{50a}$$

where

$$Z_1 = -|R_1| + iX_1 \quad . \tag{50b}$$

Because $|R_1|$ is a positive ohmic resistance and the current I_1 flows through it, there is ohmic loss which means that although the antenna performance in terms of pattern and radiation direction is preserved, the efficiency is reduced. In the case of electrically small superconducting antennas, this reduction in efficiency can be drastic.

However, all is not lost. The load Z_A can be replaced with a lossless two port as in Figure 9. The lossless matching network (S_B) is designed for matching so that

$$S_{B22} = \Gamma_2^* \quad .$$

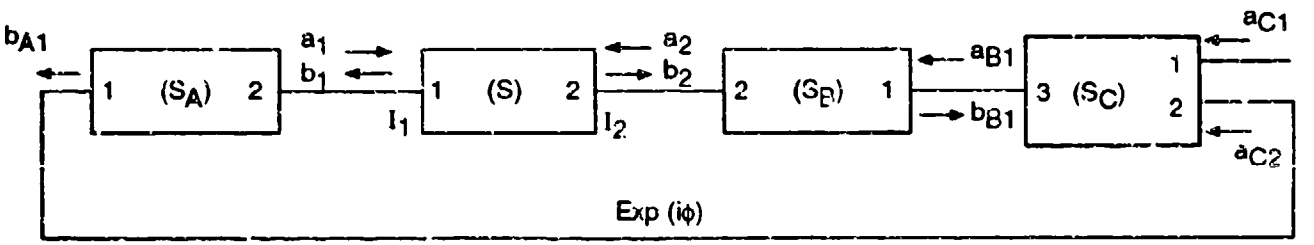

FIGURE 9. Replacing the Load Z_A With a Lossless Two Port.

Per Equation 45, while the lossless two port (S_A) is designed to produce the current I_1 with

$$S_{A22} = \frac{1}{\Gamma_1} \quad , \tag{51}$$

the output b_{A1} is fed, with the proper phase shift, to the input of a power combiner to produce the desired drive level a_{B1}.

It is not our purpose to go into the combiner details here but one way to achieve this end is to use a directional coupler with one port terminated in Z_0, with the coupling coefficients set to give zero output at the terminated port and the proper a_{B1} of the input of the matching network.

This may seem to be a somewhat complex process but if it is compared with Figure 6, one power divider and two two port matching circuits versus one power combiner, one

two port matching circuit, and one two port to meet the condition of Equation 51, the two cases are seen to be topologically equivalent.

VII. CONCLUSIONS

We have presented a detailed electromagnetic analysis of an electrically small colocated electric dipole and magnetic loop antenna array. This antenna is the simplest example of the Grimes multipole class of antenna arrays. We have determined that since the interaction term between the two elements disappears from the radial complex power, we were able to set the radial reactance to zero by choosing appropriate current magnitudes and phases on the array elements. By driving the two elements in quadrature, we saw a much increased radiation intensity and directivity as well as increased radiated power.

REFERENCES

1. K. Fujimoto, A. Henderson, K. Hirasawa, and J. R. James. *Small Antennas*. New York, Wiley, 1987.

2. R. J. Dinger, D. R. Bowling, and A. M. Martin. "A Survey of Possible Passive Antenna Applications of High Temperature Superconductors," *IEEE Trans. Microwave Theory Tech.*, Vol. MTT-39 (1991), pp 1498-1507.

3. R. C. Hansen. "Superconducting Antennas," *IEEE Trans. Aerospace Electron. Syst.*, Vol. AES-26 (1990), pp. 345-355

4. S. K. Khamas, G. G. Cook, S. P. Kingsley, R. C. Woods, and N. M. Alford. "Investigation of the Enhanced Efficiencies of Small Superconducting Loop Antenna Elements," *J. Appl. Phys.*, Vol. 74 (1993), pp. 2914-2919.

5. A. P. Pischke and H. Chaloupka. "Electrically Small Superconducting Planar Radiating Elements for Arrays," in *22nd European Microwave Conference Proceedings*, Helsinki, Finland (1992).

6. D. M. Grimes and C. A. Grimes. "Reactive Energy and Implied Antenna Capabilities," submitted to *J. Phys. D, Appl. Phys.*

7. D. M. Grimes. "A Proposed Efficient Small Antenna," 1992.

8. C. A. Grimes and D. M. Grimes. "A Small Antenna With Aerospace Application," in *1991 Aerospace Appl. Conference Digest., No. 3 , Crested Butte, Colo, 1991.*

9. D. M. Grimes. "Quantum Theory: The Classical Theory of Nonlinear Electromagnetics," *Physica D* , Vol. 32 (1988), pp. 1-17.

10. _____. "Quantum Theory and Classical, Nonlinear Electronics, *Physica D*, Vol. 20 (1986), pp. 285-302.

11. _____. "Atomic Theory and Radiative Transfer on the Basis of Nonlinear, Classical Electrodynamics," in *Essays on the Formal Aspects of Electromagnetic Theory*, River Edge, NJ, World Scientific, 1993.

12. L. J. Chu. "Physical Limitations on Omnidirectional Antennas," *J. Appl. Phys.*, Vol. 19 (1948), pp. 1163-1175.

13. R. F. Harrington. "Effect of Antenna Size on Gain, Bandwidth, and Efficiency," *J. Res. Nat. Bur. Standards D*, Vol. 64D (1960), pp. 1-12.

14. R. F. Harrington. "On the Gain and Beamwidth of Directional Antennas," *IRE Trans. on Antennas Propag.*, Vol. AP-6 (1958), pp. 219-225.

15. H. A. Wheeler. "Fundamental Limitations of Small Antennas," *Proc. IRE 35*, (1947). Pp. 1479-1331.

16. _____. "The Radiansphere Around a Small Antenna," *Proc. IRE 47*, (1959). Pp. 1325-1331.

17. C. A. Balanis. *Antenna Theory* . New York, Wiley, 1982.

18. J. D. Jackson. *Classical Electrodynamics*. 2nd ed. New York, Wiley, 1975. Chap. 16.

19. W. C. Wong. "Signal and Noise Analysis of a Loop-Monopole Active Antenna," *IEEE Trans. on Antennas Propag.*, Vol. AP-22 (1974), pp. 574-580.

20. J. A. Stratton. *Electromagnetic Theory*. New York, McGraw-Hill, 1941.

Appendix

RELATIONSHIP BETWEEN THE INSTANTANEOUS POYNTING VECTOR AND THE COMPLEX POYNTING VECTOR

It is important to recall that the complex Poynting vector can be derived directly from Maxwell's equations (Reference 20). Using standard phasor notation and $e^{i\omega t}$ time dependence

$$\nabla x \vec{E} = -i\omega\mu \vec{H} \tag{A-1a}$$

$$\nabla x \vec{H} = \vec{J} + i\omega\varepsilon \vec{E} \tag{A-1b}$$

with the complex conjugate equation for Equation A-1b as

$$\nabla x \vec{H}^* = \vec{J}^* - i\omega\varepsilon \vec{E}^* \quad . \tag{A-2}$$

Dotting $\vec{H}^*$ into Equation A-1a and $\vec{E}$ into Equation A-2, we obtain

$$\vec{H}^* \cdot \nabla x \vec{E} = -i\omega\mu \vec{H}^* \cdot \vec{H} \tag{A-3}$$

and

$$\vec{E} \cdot \nabla x \vec{H}^* = \vec{E} \cdot \vec{J}^* - i\omega\varepsilon \vec{E} \cdot \vec{E}^* \quad . \tag{A-3b}$$

Subtracting Equation A-3b from Equation A-3a, we have

$$\nabla\cdot\left(\vec{E}\,x\,\vec{H}^{*}\right)=-i\omega\left(\mu\,\vec{H}^{*}\cdot\vec{H}-\varepsilon\,\vec{E}^{*}\cdot\vec{E}\right)-\vec{E}\cdot\vec{J}^{*}\quad . \tag{A-4}$$

Allowing primed variables to denote real parts of quantities and double primes to denote imaginary parts, we can rewrite

$$\vec{H}\cdot\vec{H}^{*}=\vec{H}'^{2}+\vec{H}''^{2} \tag{A-5a}$$

and

$$\vec{E}\cdot\vec{E}^{*}=\vec{E}'^{2}+\vec{E}''^{2} \tag{A-5b}$$

which have no imaginary parts.

However, $\vec{E}$ x $\vec{H}^{*}$ does have an imaginary part. Thus

$$\vec{E}\,x\,\vec{H}^{*}=\left(\vec{E}'x\vec{H}'+\vec{E}''x\vec{H}''\right)+i\left(\vec{E}'x\vec{H}''-\vec{E}''x\vec{H}'\right) \tag{A-6}$$

while

$$\vec{E}\cdot\vec{J}=\vec{E}^{*}\cdot\sigma\vec{E}^{*} \tag{A-7}$$

and as long as the conductivity, σ, is real, $\vec{E}\cdot\vec{J}^{*}$ is a purely real quantity. So returning to Equation (A-4),

$$\nabla\cdot\left(\vec{E}\,x\,\vec{H}^{*}\right)=\nabla\cdot\left[\left(\vec{E}'x\vec{H}'+\vec{E}''x\vec{H}''\right)+i\left(\vec{E}'x\vec{H}''-\vec{E}''x\vec{H}'\right)\right]$$

$$=\nabla\cdot\left[\mathrm{Re}\left(\vec{E}\,x\,\vec{H}^{*}\right)+i\,\mathrm{Im}\left(\vec{E}\,x\,\vec{H}^{*}\right)\right]\quad . \tag{A-8}$$

Using Equation A-8 with Equation A-4,

$$\frac{1}{2}\nabla \cdot \mathrm{Re}\left(\vec{E} \times \vec{H}^*\right) = \frac{1}{2}\left(\vec{E} \cdot \vec{J}^*\right) \tag{A-9a}$$

and

$$\frac{1}{2}\nabla \cdot \mathrm{Im}\left(\vec{E} \times \vec{H}^*\right) = -\omega\left(\mu \frac{\vec{H} \cdot \vec{H}^*}{2} - \frac{\vec{E} \cdot \vec{E}^*}{2}\right) \quad . \tag{A-9b}$$

Integrating Equations A-9 over a sphere of volume V with boundary S, we see that

$$\frac{1}{2}\int_V \nabla \cdot \mathrm{Re}\left(\vec{E} \times \vec{H}^*\right) dV = -\frac{1}{2}\int_V \vec{E} \cdot \vec{J}^* dV \tag{A-10a}$$

and

$$\frac{1}{2}\int_V \nabla \cdot \mathrm{Im}\left(\vec{E} \times \vec{H}^*\right) dV = -\omega \int_V \left(\mu \frac{\vec{H} \cdot \vec{H}^*}{2} - \frac{\vec{E} \cdot \vec{E}^*}{2}\right) dV \quad . \tag{A-10b}$$

Of course, the above can be found in many text books and we repeat it here for the reader's convenience.

Now let the instantaneous Poynting vector be given by

$$\vec{\mathbf{S}} = \vec{\mathbf{E}} \times \vec{\mathbf{H}} \tag{A-11}$$

where all boldface variables indicate instantaneous quantities. $\vec{S}$ is a power density, i.e. power/unit area and has the MKS units of watts/m^2. The total power crossing some closed surface at a given time is found by integrating the normal component of $\vec{S}$ over the entire surface, or

$$\mathbf{P} = \oiint_S \vec{\mathbf{S}} \cdot d\vec{s} = \oiint_S \vec{\mathbf{S}} \cdot \hat{n} da \tag{A-12}$$

where **P** is the instantaneous power in watts. We can write $\vec{\mathbf{E}}$ and $\vec{\mathbf{H}}$ in the form (Reference 17)

$$\vec{\mathbf{E}}(x,y,z;t) = \mathrm{Re}\left[\vec{E}(x,y,z)e^{i\omega t}\right] \tag{A-13a}$$

$$\vec{\mathbf{H}}(x,y,z;t) = \mathrm{Re}\left[\vec{H}(x,y,z)e^{i\omega t}\right] \tag{A-13b}$$

and then

$$\vec{\mathbf{E}} = \vec{E}' \cos \omega t + \vec{E}'' \sin \omega t \tag{A-14a}$$

and

$$\vec{\mathbf{H}} = \vec{H}' \cos \omega t + \vec{H}'' \sin \omega t \quad , \tag{A-14b}$$

d we have thrown away all else. Using Equations A-14, the instantaneous Poynting ·-tor becomes

$$\vec{\mathbf{S}} = \left(\vec{E}' x \vec{H}'\right)\cos^2 \omega t + \left(\vec{E}' x \vec{H}'' + \vec{E}'' x \vec{H}'\right)\sin \omega t \cos \omega t + \left(\vec{E}'' x \vec{H}''\right)\sin^2 \omega t \quad . \tag{A-15}$$

An alternate form of Equation A-15 is

$$\vec{S} = \frac{1}{2}\left(\vec{E}' x \vec{H}' + \vec{E}'' x \vec{H}''\right) + \frac{1}{2}\left(\vec{E}' x \vec{H}'' + \vec{E}'' x \vec{H}'\right)\sin 2\omega t$$

$$+ \frac{1}{2}\left(\vec{E}' x \vec{H}' - \vec{E}'' x \vec{H}''\right)\cos 2\omega t \qquad \text{(A-16)}$$

or

$$\vec{S} = \vec{N}_0 + \vec{N}_1 \cos 2\omega t + \vec{N}_2 \sin 2\omega t \qquad \text{(A-17)}$$

where

$$\vec{N}_0 = \frac{1}{2}\left(\vec{E}' x \vec{H}' + \vec{E}'' x \vec{H}''\right) \qquad \text{(A-18a)}$$

$$\vec{N}_1 = \frac{1}{2}\left(\vec{E}' x \vec{H}' - \vec{E}'' x \vec{H}''\right) \qquad \text{(A-18b)}$$

$$\vec{N}_2 = \frac{1}{2}\left(\vec{E}' x \vec{H}'' + \vec{E}'' x \vec{H}'\right) \qquad \text{(A-18c)}$$

which is Grimes' notation (Reference 6).

Once we time average Equation A-17 over one period, τ, we find that the integrals over cos 2 ωt and sin 2ωt are zero. Thus while

$$\vec{S}_{avg} = \vec{S} = \vec{N}_0 = \mathrm{Re}\left(\vec{E} x \vec{H}^*\right) \quad , \qquad \text{(A-19)}$$

the terms containing $\vec{N}_1$ and $\vec{N}_2$ average to zero. Then the radiated power is also the time averaged power, as usual,

$$P_{rad} = P_{avg} = \oiint_A \frac{1}{2}\mathrm{Re}\left(\vec{E} \times \vec{H}^*\right) \cdot \hat{n}da = \oiint_A \vec{N}_0 \cdot \hat{n}da \quad . \tag{A-20}$$

Only the instantaneous total power keeps the $\vec{N}_1$ and $\vec{N}_2$ terms. Thus

$$\mathbf{P} = \oiint_A \vec{\mathbf{S}} \cdot \hat{n}da$$

$$= \oiint_A \vec{N}_0 \cdot \hat{n}da + \cos 2\omega t \oiint_A \vec{N}_1 \cdot \hat{n}da + \sin 2\omega t \oiint_A \vec{N}_1 \cdot \hat{n}da \quad . \tag{A-21}$$

But neither $\vec{N}_1$ nor $\vec{N}_2$, given in Equations A-18b and A-18c are equal to $\frac{1}{2}\,\mathrm{Im}(\vec{E} \times \vec{H}^*)$, which is

$$\frac{1}{2}\mathrm{Im}\left(\vec{E} \times \vec{H}^*\right) = \frac{1}{2}\left(\vec{E}' \times \vec{H}'' - \vec{E}'' \times \vec{H}'\right) \tag{A-22}$$

which is obtained from Maxwell's equations and their associated complex conjugates. Thus there is no explicit relationship between the imaginary part of the complex Poynting vector and the instantaneous Poynting vector.

INITIAL DISTRIBUTION

4 Chief of Naval Research, Arlington
  ONR-312
    Dr. D. H. Liebenberg (1)
    Dr. I. Mack (1)
    Dr. Y. S. Park (1)
  ONR-332, Dr. W. Smith (1)
1 Naval Command Control and Ocean Surveillance Center RDTE Division, San Diego
  (R. Dinger)
2 Defense Technical Information Center, Alexandria
5 Comarco, Incorporated, Ridgecrest, CA (D. White)
1 Crale, Incorporated, State College, PA (D. M. Grimes)
1 Southwall Technologies, Palo Alto, CA (C. Grimes)
2 University of Sheffield, England
  G. Cook (1)
  S. Khamas (1)

ON-SITE DISTRIBUTION

1 Code C02
4 Code C0223 (3 plus Archives copy)
1 Code C023
1 Code C0231, J. Stanford
2 Code C02313
    H. Brooks (1)
    S. Chesnut (1)
8 Code C02316
    D. Banks (1)
    D. Bowling (5)
    D. Decker (1)
    A. Martin (1)
11 Code C02318
    D. Marrs (1)
    P. Overfelt (10)
1 Code C253, B. Bailey
1 Code C28203, J. Mosko
2 Code C2822
    T. Hoppus (1)
    M. Neel (1)
1 Code C2901A, D. Burdick
3 Code C2953
    M. Fortune (1)
    D. Marvin (1)
    D. Paolino (1)
6 Code C2951
    J. Butterworth (1)
    R. Chew (1)
    L. Hagman (1)
    M. Sanders (1)
    R. Skatvold (1)
    H. Wang (1)
5 Code C2952
    M. Afendykiw (1)
    K. Doan (1)
    S. Gaaleb (1)
    M. Whitham (1)
    T. Williams (1)
2 Code C3931
    D. Purdy (1)
    W. Swinford (1)